Korean J. Chem. Eng., 33(11), 3207-3215 (2016)
DOI: 10.1007/s11814-016-0162-y

pISSN: 0256-1115
eISSN: 1975-7220

Regenerable potassium-based alumina sorbents prepared by CO_2 thermal treatment for post-combustion carbon dioxide capture

Seong Bin Jo*,‡, Soo Chool Lee,‡, Ho Jin Chae*, Min Sun Cho*, Joong Beom Lee***, Jeom-In Baek***, and Jae Chang Kim*,†**

*Department of Chemical Engineering, Kyungpook National University, Daegu 41566, Korea
**Research Institute of Advanced Energy Technology, Kyungpook National University, Daegu 41566, Korea
***Korea Electric Power Research Institute, Daejeon 34056, Korea
(*Received 2 March 2016 • accepted 13 June 2016*)

Abstract−Potassium carbonate supported on alumina is used as a solid sorbent for CO_2 capture at low temperatures. However, its CO_2 capture capacity decreases immediately after the first cycle. This regeneration problem is due to the formation of the by-product [$KAl(CO_3)(OH)_2$] during CO_2 sorption. To overcome this problem, a new regenerable potassium-based sorbent was fabricated by CO_2 thermal treatment of sorbents prepared by the impregnation of δ-alumina with K_2CO_3 in the presence of 10 vol% CO_2 and 10 vol% H_2O. The CO_2 capture capacities of the new regenerable sorbents were maintained over multiple CO_2 sorption tests. These results can be explained by the fact that the sorbent prepared by CO_2 thermal treatment did not form any by-product during CO_2 sorption. Based on these results, we suggest that the regeneration properties of potassium-based sorbents using δ-alumina could be significantly improved by the use of the CO_2 thermal treatment developed in this study.

Keywords: CO_2, Dry Sorbent, $KAl(CO_3)(OH)_2$, CO_2 Thermal Treatment, Regeneration

INTRODUCTION

Carbon dioxide (CO_2) is a major greenhouse gas that is released into the atmosphere as a result of the combustion of fossil fuels (oil, natural gas and coal), causing global warming, which may have a disastrous effect on the environment [1-3]. It can be removed from flue gas and waste gas streams by various methods, including membrane separation, absorption with a solvent and adsorption using molecular sieves [4-17]. However, these methods are costly and consume large amounts of energy. One of the more efficient techniques for the removal of CO_2 is its chemical absorption using a dry regenerable alkali-metal carbonate-based solid sorbent (M_2CO_3, where M=K, Na), which is a cost-effective and energy-efficient way of capturing CO_2 from flue gas [18-30]. In the absorption process, the alkali-metal carbonate reacts with the CO_2 and water vapor at 40-80 °C, forming an alkali-metal bicarbonate ($M_2CO_3+H_2O+CO_2=2MHCO_3$) [18,22-25]. Several studies have found that when using cyclic CO_2 sorption systems under moist conditions, K_2CO_3 is the best performing alkali-metal carbonate [19,24-28]. However, a common problem is that the overall carbonation reaction using alkali-metal carbonates is rather slow. Many attempts have been made to resolve this, such as by dispersing the active alkali-metal carbonate by supporting it on a porous material such as activated carbon, TiO_2, ZrO_2, silica gel or Al_2O_3, which enhances the sorption rate and provides the attrition resistance required for use in a fluid bed or transport reactor [21,24-37]. Nevertheless, such sorbents have a disadvantage in that their reactivity always decreases with increases in the sorption/regeneration operations [38-46].

Several previous studies have attempted to overcome the deactivation of potassium-based alumina sorbents. Zhao et al. investigated the regeneration behavior of K_2CO_3/Al_2O_3 in detail using a thermogravimetric analysis-Fourier transform infrared spectroscopy (TGA-FTIR) system. The regeneration process of K_2CO_3/Al_2O_3 consists of three steps as the temperature increases and the material could be completely regenerated in various atmospheres such as pure N_2, pure CO_2 and CO_2/H_2O, with a final temperature of 300 °C [47]. Other studies have shown the performance of regenerable potassium-based alumina sorbents under various conditions [48-50]. However, all of these sorbents required a high regeneration temperature greater than 250 °C, as a result of the formation of a by-product [$KAl(CO_3)(OH)_2$], which did not completely revert to the original K_2CO_3 phase after regeneration at 200 °C. The deactivation problem could be solved using a potassium-based alumina sorbent with α-alumina as the support material, despite the slow sorption rate compared to other sorbents using γ and δ-alumina [40-41]. In another study, a regenerable potassium-based sorbent was prepared by the impregnation of modified γ-alumina with K_2CO_3 [51]. However, at present, the sorption and regeneration properties of potassium-based alumina sorbents using δ-alumina have not yet been sufficiently studied.

In this study, new regenerable potassium-based alumina sorbents were prepared by CO_2 thermal treatment after the impregnation of

†To whom correspondence should be addressed.
E-mail: kjchang@knu.ac.kr
‡Seong Bin Jo and Soo Chool Lee contributed equally to this work.
‡This article is dedicated to Prof. Seong Ihl Woo on the occasion of his retirement from KAIST.

δ-alumina (instead of γ-alumina) with 30, 40 and 50 wt% K_2CO_3, to overcome the deactivation problem associated with δ-alumina. The CO_2 capture capacities of the regenerable potassium-based δ-alumina were investigated during multiple cycles in the presence of 1 vol% CO_2 and 10 vol% H_2O in a fixed-bed reactor. In addition, the physical properties of the new regenerable potassium-based alumina sorbents were investigated using X-ray diffraction (XRD), ultra-high resolution field emission scanning electron microscopy (UHR-FE-SEM), Brunauer-Emmett-Teller (BET) analysis, thermogravimetric analysis (TGA) and temperature programmed desorption (TPD).

EXPERIMENTAL

1. Preparation of Sorbents

Regenerable potassium-based alumina sorbents were prepared using a novel preparation method. The preparation of the sorbents consisted of three steps: (1) the precipitation of alumina, (2) impregnation of alumina with K_2CO_3 and (3) CO_2 thermal treatment.

1-1. Precipitation of δ-Alumina

Al_2O_3 was prepared by precipitation using aluminum nitrate nonahydrate ($Al(NO_3)_3{\cdot}9H_2O$, Aldrich, 99.9%) and sodium hydroxide (NaOH, Duksan). Aluminum nitrate was added to deionized (DI) water at a level of 0.5 M. The solution was then adjusted by the dropwise addition of 1.5 M of NaOH until the pH reached 10. The resulting precipitate was aged for 12 h in the solution at room temperature. The product was washed sufficiently with DI water and dried. The resulting Al_2O_3 was then calcined in an electric muffle furnace under air at 950 °C for 4 h.

1-2. Impregnation of Alumina with K_2CO_3

The impregnation procedure for supporting the K_2CO_3 on alumina was as follows: alumina was added to a solution containing the desired ratio of anhydrous potassium carbonate in DI water and then mixed with a magnetic stirrer for 24 h at room temperature. After stirring, the mixture was dried in a rotary evaporator at 40-60 °C. The dried samples were calcined in a furnace under N_2 at 500 °C for 4 h, with the temperature ramping at a rate of 3 °C/min.

1-3. CO_2 Thermal Treatment of Sorbent

The CO_2 thermal treatment was used to form the $KAl(CO_3)(OH)_2$ phase to enhance the regeneration properties of the potassium-based alumina sorbents. In the presence of 10 vol% CO_2 and 10 vol% H_2O, the impregnated powder was heat-treated using the following temperature program: (1) holding at 60 °C for 2 h, (2) ramping the temperature to 200 °C at a rate of 1 °C/min and (3) holding at 200 °C for 3 h.

The resulting potassium-based alumina sorbents were denoted as KAl(D)INT, where K represents the potassium carbonate (K_2CO_3), Al(D) represents the δ-alumina support material, I represents the impregnation method, N represents the loading of potassium carbonate (wt%) and T represents the CO_2 thermal treatment method. For example, KAl(D)I40 is the potassium-based alumina sorbent prepared by the impregnation of δ-alumina with 40 wt% K_2CO_3 and KAl(D)I40T is the sorbent prepared by the CO_2 thermal treatment of the KAl(D)I40 sorbent.

2. Characterization

2-1. Physico-chemical Characterization

The crystal structures of the adsorbents were analyzed by using a Cu Ka radiation source in a Phillips XPERT X-ray diffraction (XRD) unit at the Korea Basic Science Institute in Daegu. Nitrogen adsorption-desorption isotherms at −196 °C were measured with a Micromeritics ASAP 2020 instrument to acquire the textural properties of the materials. UHR-FE-SEM (Hitachi, S-4800) was performed to identify the crystalline phases and morphologies of the materials at the Korea Basic Science Institute in Daegu. The amount of potassium carbonate impregnated was measured using inductively coupled plasma atomic emission spectroscopy (ICP-AES; Thermo, Thermo Jarrell Ash IRISAP) with the following process. First, the K_2CO_3 dispersed on alumina was dissolved using DI water and stirring and then the resulting solution was analyzed using ICP-AES.

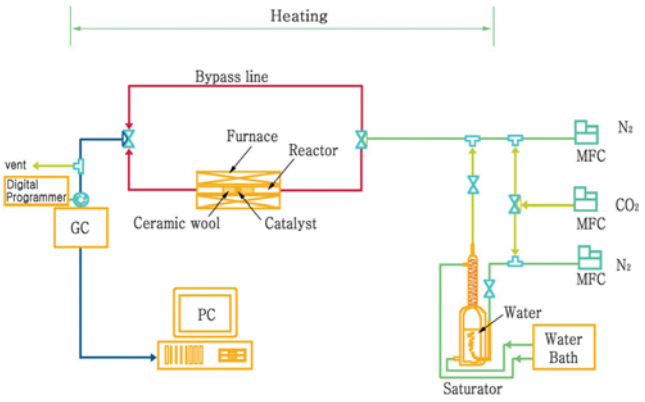

Fig. 1. Schematic of packed bed system used for CO_2 absorption and regeneration experiments.

2-2. Absorption and Regeneration Tests

The CO_2 absorption and regeneration processes were determined by monitoring the CO_2 concentration using gas chromatography (GC), as schematically shown in Fig. 1. The sorbent (0.5 g) was packed into a fixed-bed reactor with a diameter of 1 cm. The fixed-bed reactor was placed in an electric furnace at atmospheric pressure. To prevent the condensation of water vapor, the inlet and outlet lines of the reactor were maintained at temperatures above 100 °C using heating tape before the injection of gas into the reactor and GC column. A 1/8 in. stainless tube packed with Porapak Q was used as the column. The outlet gases from the reactor were analyzed automatically every 4 min with a thermal conductivity detector (TCD; Donam Systems Inc.) equipped with an auto sampler (Valco Instruments Co. Inc.). First, feed gas (1 vol% CO_2, 10 vol% H_2O and balance N_2 at 40 ml/min) was passed through the bed at the absorption temperature of 60 °C. When the CO_2 concentration of the outlet gas reached the same level as that of the inlet CO_2 feed gas (1 vol%) in the CO_2 absorption process, the gas composition was changed from the feed gas to pure nitrogen to purge the CO_2 gas in the reactor. After the concentration of CO_2 decreased to zero, the temperature was increased to 200 °C to regenerate the spent sorbents.

RESULTS AND DISCUSSION

1. Potassium-based Alumina Sorbent

Fig. 2 shows the CO_2 capture capacities of the KAl(D)I30,

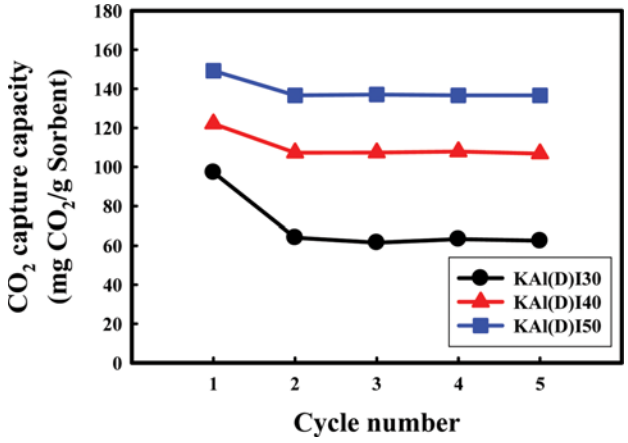

Fig. 2. CO_2 capture capacities of KAl(D)I30, KAl(D)I40 and KAl(D)I50 in the presence of 1 vol% CO_2 and 10 vol% H_2O, with sorption being performed at 60 °C and regeneration at 200 °C.

KAl(D)I40 and KAl(D)I50 sorbents over multiple cycles, with the sorption performed at 60 °C and regeneration at 200 °C, in the presence of 1 vol% CO_2 and 10 vol% H_2O. The KAl(D)I30, KAl(D)I40 and KAl(D)I50 sorbents were prepared by the impregnation of δ-alumina with 30, 40 and 50 wt% K_2CO_3, respectively, to investigate the effects of the K_2CO_3 loading. The CO_2 capture capacities were calculated from the breakthrough curves for each cycle and the values at the first cycle were 97.2, 122.1 and 149.2 mg CO_2/g sorbent for KAl(D)I30, KAl(D)I40 and KAl(D)I50, respectively. However, as shown in Fig. 2, the CO_2 capture capacities of the sorbents decreased for the second cycle and stayed roughly the same after this. Fig. 3 shows the breakthrough curves of the KAl(D)I30, KAl(D)I40 and KAl(D)I50 sorbents at 1 and 5 cycles in the pres-

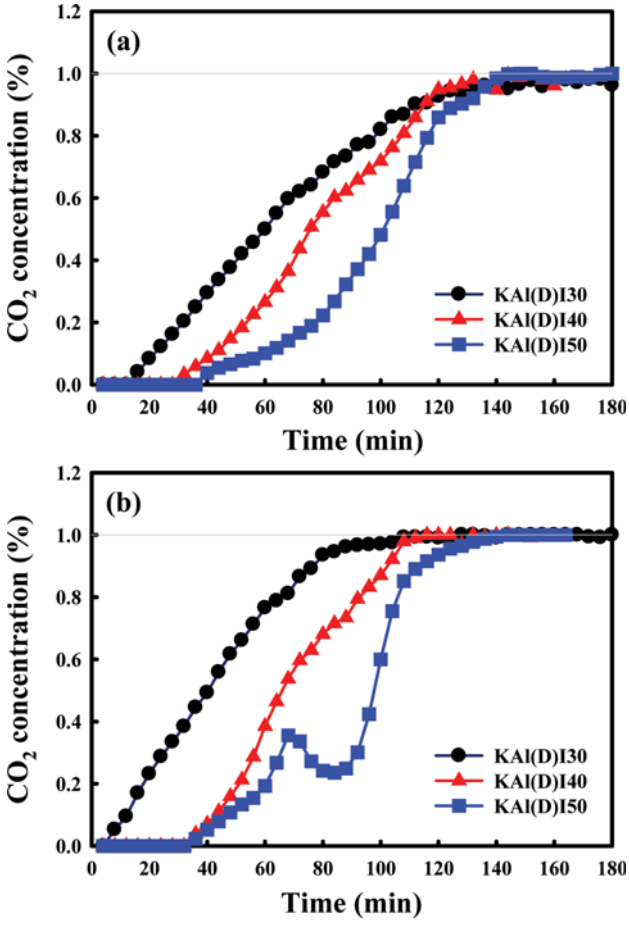

Fig. 3. Breakthrough curves of KAl(D)I30, KAl(D)I40 and KAl(D)I50 at 60 °C in the presence of 1 vol% CO_2 and 10 vol% H_2O after (a) 1 and (b) 5 cycles.

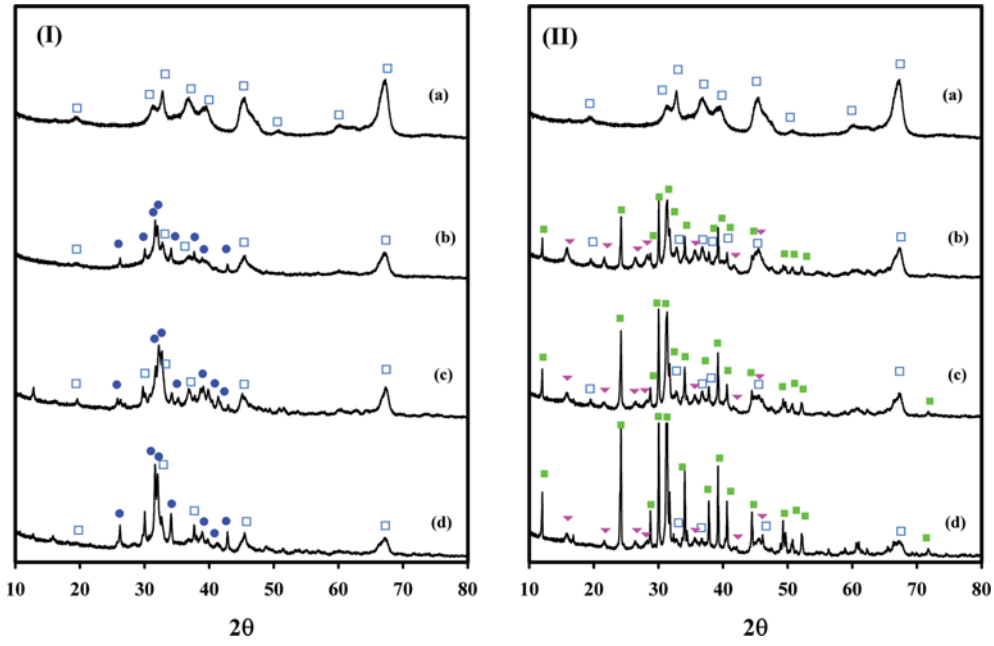

Fig. 4. XRD patterns of (a) δ-alumina, (b) KAl(D)I30, (c) KAl(D)I40 and (d) KAl(D)I50 sorbents (I) before and (II) after CO_2 sorption; (□) δ-Al_2O_3; (●) K_2CO_3; (■) $KHCO_3$; (▼) $KAl(CO_3)(OH)_2$.

ence of 1 vol% CO_2 and 10 vol% H_2O at 60 °C. In case of the bare δ-alumina, its breakthrough curve was excluded because the δ-alumina had no CO_2 capture capacity. The breakthrough times during the first cycle were approximately 16, 32 and 40 min, respectively. In the fifth cycle, the breakthrough time of KAl(D)I30 was reduced from 16 min to 4 min, whereas the values for KAl(D)I40 and KAl(D)I50 were almost similar to those at the first cycle. However, the CO_2 capture capacities of KAl(D)I40 and KAl(D)I50 decreased from 122.1 to 107.3 and 149.2 to 136.7, respectively. From these results, it must be noted that the deactivation of the sorbent reduced with increasing K_2CO_3 loading.

To investigate the reason for the deactivation of the potassium-based δ-alumina sorbents, the structures of the sorbents before and after CO_2 sorption were examined using XRD (Fig. 4). The XRD patterns of the alumina materials calcined at 950 °C showed the δ-alumina phase (JCPDS No. 46-1131). The XRD patterns of the fresh KAl(D)I30, KAl(D)I40 and KAl(D)I50 sorbents showed the K_2CO_3 and δ-alumina phases. On the other hand, the XRD patterns of these sorbents after the CO_2 sorption showed the δ-alumina phase, $KHCO_3$ phase (JCPDS No. 70-0995) and $KAl(CO_3)(OH)_2$ phase (JCPDS No. 22-0791). This means that the deactivation of the potassium-based δ-alumina sorbents was affected by the formation of $KAl(CO_3)(OH)_2$, as reported elsewhere [39-42].

To understand the regeneration properties of the sorbents in detail, TPD tests were performed on KAl(D)I30, KAl(D)I40 and KAl(D)I50 after the CO_2 sorption at 60 °C. These tests were carried out by measuring the concentration of CO_2 desorbed while the temperature was increasing at a rate of 1 °C/min. As shown in Fig. 5, the TPD profiles of the sorbents showed two types of CO_2 desorption peaks, resulting from the $KHCO_3$ and $KAl(CO_3)(OH)_2$ produced during the CO_2 sorption [39,40,51]. The initial peak at around 130 °C occurred as a result of the desorption of CO_2 from the decomposition of $KHCO_3$. The second peak at 270 °C occurred because of the conversion of $KAl(CO_3)(OH)_2$ into K_2CO_3 and Al_2O_3 [39-42,51]. The first CO_2 peak increased with increasing K_2CO_3 loading, whereas the second CO_2 peak decreased. Importantly, the amount of $KAl(CO_3)(OH)_2$, which acted as an inactive material, was observed to decrease with increases in the amount of K_2CO_3. The regeneration and desorption capacities of the KAl(D)I30, KAl(D)I40 and KAl(D)I50 sorbents are summarized in Table 1. The regeneration capacities were calculated from the C_5/C_1 ratio, in which C_1 and C_5 represent the CO_2 capture capacities at 1 and 5 cycles, respectively. The desorption capacities were calculated from the peak areas observed in the TPD profiles (Fig. 5). The regeneration capacities were 65.3%, 88.3% and 91.3% for KAl(D)I30, KAl(D)I40 and KAl(D)I50, respectively, indicating that the regeneration capacity was affected by the amount of alumina. As listed in Table 1, the desorption capacity calculated from the TPD peak area at 270 °C decreased with decreasing alumina content. These results agree quantitatively with the difference between the CO_2 capture capacities at 1 and 5 cycles (C_1-C_5). It is clear that a by-product such as $KAl(CO_3)(OH)_2$ contributed to the deactivation of the potassium-based alumina sorbents. Based on these results, the deactivation of potassium-based sorbents using alumina as a support can be reduced by increasing the loading of K_2CO_3.

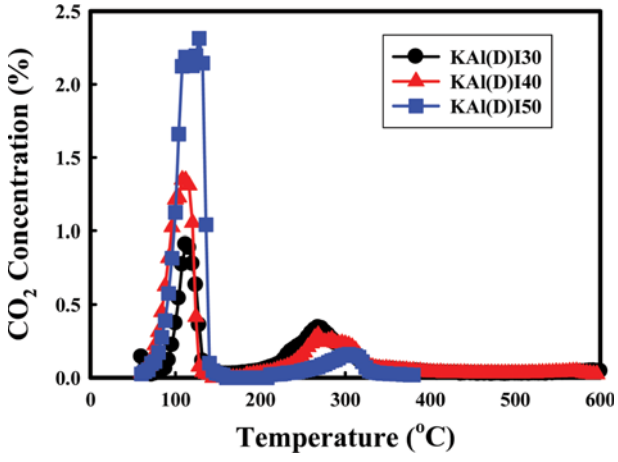

Fig. 5. TPD profiles of KAl(D)I30, KAl(D)I40 and KAl(D)I50 sorbents after CO_2 sorption.

2. New Regenerable Potassium-based Alumina Sorbents with CO_2 Thermal Treatment

The fundamental problem with the regeneration of potassium-based alumina sorbents could not be completely resolved at a regeneration temperature of 200 °C, because the by-product [$KAl(CO_3)(OH)_2$] was completely converted to the original K_2CO_3 phase at temperatures above 300 °C. To overcome this problem, a new potassium-based alumina sorbent was required. Fig. 6 shows the XRD patterns of the KAl(D)I40 sorbent after regeneration at 200 °C and 300 °C. The XRD pattern after the regeneration at 200 °C shows the presence of both K_2CO_3 and $KAl(CO_3)(OH)_2$, indicating that only $KHCO_3$ was completely converted to the original phase. After the regeneration at 300 °C, only the K_2CO_3 peaks are observed in the XRD patterns. These results are in good agreement with the TPD results. Our previous paper reported that the new potassium sorbent, which was prepared by the impregnation of a modified alumina support containing $KAl(CO_3)(OH)_2$ with K_2CO_3, had a high CO_2 capture capacity and excellent regeneration properties even at 130 °C, in spite of the use of alumina as a support [42]. Of

Table 1. Sorption and desorption performances of potassium-based alumina sorbents

Sample	Sorption capacity calculated from breakthrough curves (mg CO_2/g sorbent)			Regeneration capacity (%)	Desorption capacity calculated from TPD results (mg CO_2/g sorbent)	
	Cycle 1 (C_1)	Cycle 5 (C_5)	C_1-C_5	$C_5/C_1\times100$	130 °C	270 °C
KAl(D)I30	97.2	62.5	34.7	64.3	62.6	34.6
KAl(D)I40	122.1	106.8	15.3	87.5	98.7	17.5
KAl(D)I50	149.2	136.6	12.6	91.6	133.2	13.3

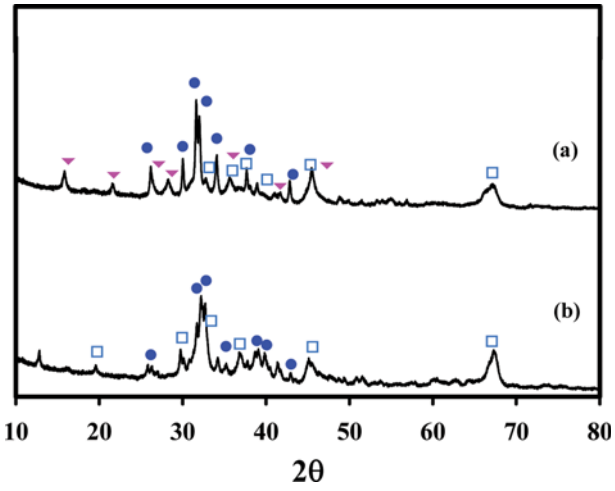

Fig. 6. XRD patterns of KAl(D)I40 sorbent after regeneration at (a) 200 and (b) 300 °C under N_2. (□) δ-Al_2O_3; (●) K_2CO_3; (▼) $KAl(CO_3)(OH)_2$.

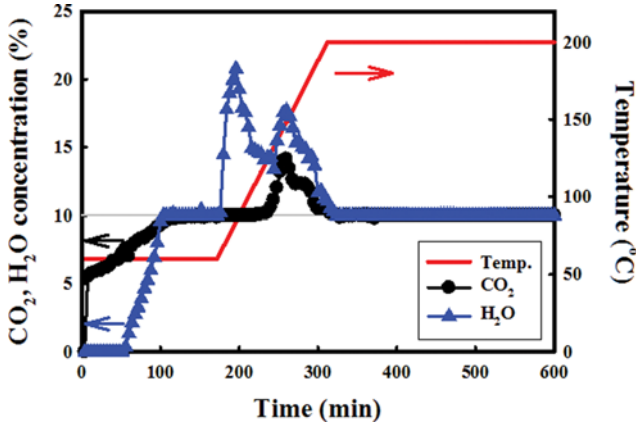

Fig. 7. Behavior of CO_2 and H_2O during CO_2 thermal treatment in the presence of 10 vol% CO_2 and 10 vol% H_2O.

note is that the $KAl(CO_3)(OH)_2$ remained in the sorbent when it was calcined at temperatures below 200 °C after CO_2 sorption at 60 °C, indicating that the regeneration problem could be completely resolved by the CO_2 thermal treatment previously reported by our group. Based on these results, the new regenerable sorbents were prepared using the CO_2 thermal treatment method discussed in the experimental section. It was important that the potassium-based alumina sorbent prepared by the impregnation of δ-alumina with K_2CO_3 be held at 60 °C for 2 h in the presence of 10 vol% CO_2

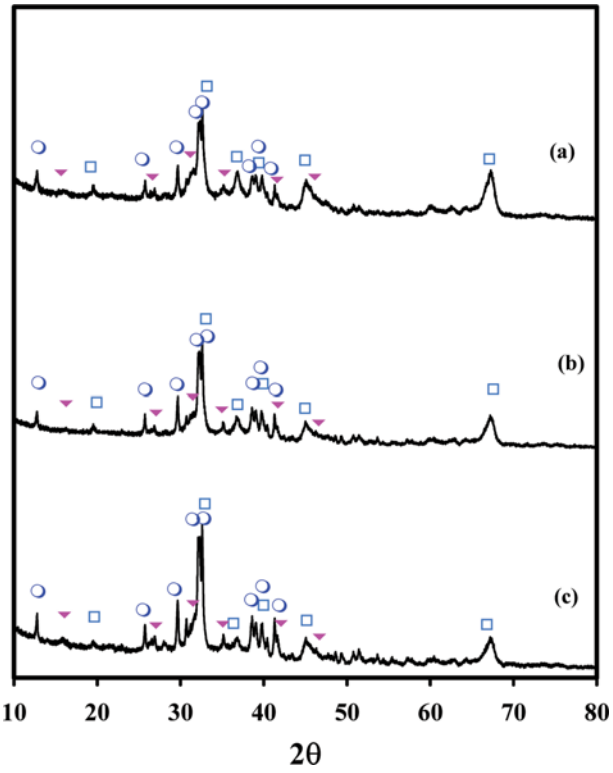

Fig. 8. XRD patterns of fresh (a) KAl(D)I30T, (b) KAl(D)I40T and (c) KAl(D)I50T sorbents; (□) δ-Al_2O_3; (○) K_2CO_3·1.5H_2O; (▼) $KAl(CO_3)(OH)_2$.

and 10 vol% H_2O, followed by thermal treatment for 3 h at 200 °C using the same gas conditions.

To monitor the behavior of CO_2 and H_2O during the CO_2 thermal treatment, the concentrations of CO_2 and H_2O were measured under the same CO_2 thermal treatment conditions. Fig. 7 shows the behavior of CO_2 and H_2O during the CO_2 thermal treatment in the presence of 10 vol% CO_2 and 10 vol% H_2O. The KAl(D)I40 sorbent absorbed CO_2 and H_2O at 60 °C. In addition, the CO_2 and H_2O gases desorbed at temperatures above 130 °C and 60 °C, respectively. Fig. 8 shows the XRD patterns of the fresh KAl(D)I30T, KAl(D)I40T and KAl(D)I50T sorbents prepared using the CO_2 thermal treatment method. As expected, the XRD patterns of all the fresh potassium-based alumina sorbents showed the δ-alumina (JCPDS No. 46-1131), K_2CO_3·1.5H_2O (JCPDS No. 73-0470) and $KAl(CO_3)(OH)_2$ peaks (JCPDS No. 22-0791), with no $KHCO_3$ being observed. Note that $KAl(CO_3)(OH)_2$ was observed in the XRD patterns after the CO_2 thermal treatment of the sorbent. This

Table 2. Textural properties of alumina and potassium-based alumina sorbents

Sample name	Surface area (m^2/g)	Pore volume (cm^3/g)	Average pore size (nm)	Sample name	Surface area (m^2/g)	Pore volume (cm^3/g)	Average pore size (nm)
Al_2O_3-950	101.8	0.34	13.1	Al_2O_3-950T	109.4	0.31	11.2
KAl(D)I30	42.5	0.14	13.4	KAl(D)I30T	31.0	0.12	15.5
KAl(D)I40	34.0	0.12	14.0	KAl(D)I40T	27.3	0.12	16.4
KAl(D)I50	21.6	0.10	19.1	KAl(D)I50T	19.5	0.07	13.8

means that the $KHCO_3$ produced during the CO_2 sorption was completely converted into $K_2CO_3 \cdot 1.5H_2O$, which is an active material, during the CO_2 thermal treatment in the presence of water vapor. From these results, we found that potassium-based sorbents containing $KAl(CO_3)(OH)_2$ could easily be prepared using the CO_2 thermal treatment method.

Table 2 lists textural properties such as the surface area, pore volume and average pore size of the δ-alumina, KAl(D)I30T, KAl(D)I40T and KAl(D)I50T sorbents with and without the CO_2 thermal treatment. The bare δ-alumina showed a surface area of 101.8 m^2/g, a pore volume of 0.34 cm^3/g and an average pore size of 13.1 nm. The surface area and pore volume of the potassium-based alumina sorbents without the CO_2 thermal treatment decreased with an increase in the K_2CO_3 loading. The δ-alumina with the CO_2 thermal treatment showed a surface area of 109.4 m^2/g, a pore volume of 0.31 cm^3/g and an average pore size of 11.2 nm, indicating that the CO_2 thermal treatment had no influence on the textural properties of δ-alumina. On the other hand, the textural properties of the sorbents with the CO_2 thermal treatment decreased compared with the sorbents without the CO_2 thermal treatment. Based on these results, it is thought that the pore volumes and surface areas of the potassium-based δ-alumina sorbents with the CO_2 thermal treatment decreased in comparison with the sorbents without the CO_2 thermal treatment.

Fig. 9 shows SEM images of the δ-alumina, KAl(D)I30T, KAl(D)I40T and KAl(D)I50T sorbents. The alumina, which was prepared using the precipitation method, formed nanoparticles with a diameter of approximately 50 nm. The potassium-based δ-alumina sorbents prepared using the CO_2 thermal treatment showed good K_2CO_3 doping on the surface of the alumina materials. In addition, some nanorods were observed among the agglomerates and the number of these decreased as the amount of K_2CO_3 increased.

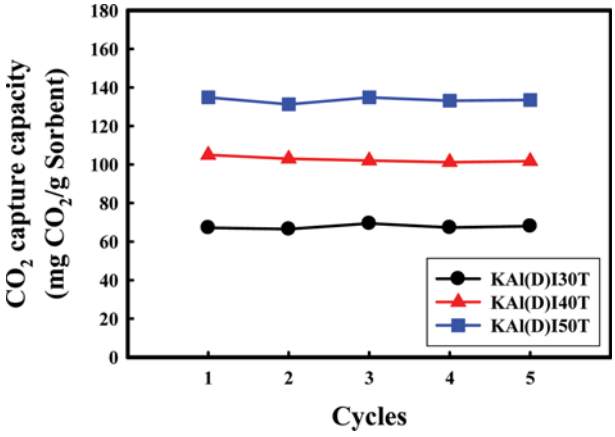

Fig. 10. CO_2 capture capacities of KAl(D)I30T, KAl(D)I40T and KAl(D)I50T sorbents in the presence of 1 vol% CO_2 and 10 vol% H_2O, with sorption being performed at 60 °C and regeneration at 200 °C.

Fig. 10 shows the CO_2 capture capacities of the KAl(D)I30T, KAl(D)I40T and KAl(D)I50T sorbents prepared using the CO_2 thermal treatment in the presence of 1 vol% CO_2 and 10 vol% H_2O at 60 °C. As shown in Fig. 10, the potassium-based alumina sorbents prepared using the CO_2 thermal treatment method showed CO_2 capture capacities of 67.2, 105.0 and 134.9 mg CO_2/g sorbent

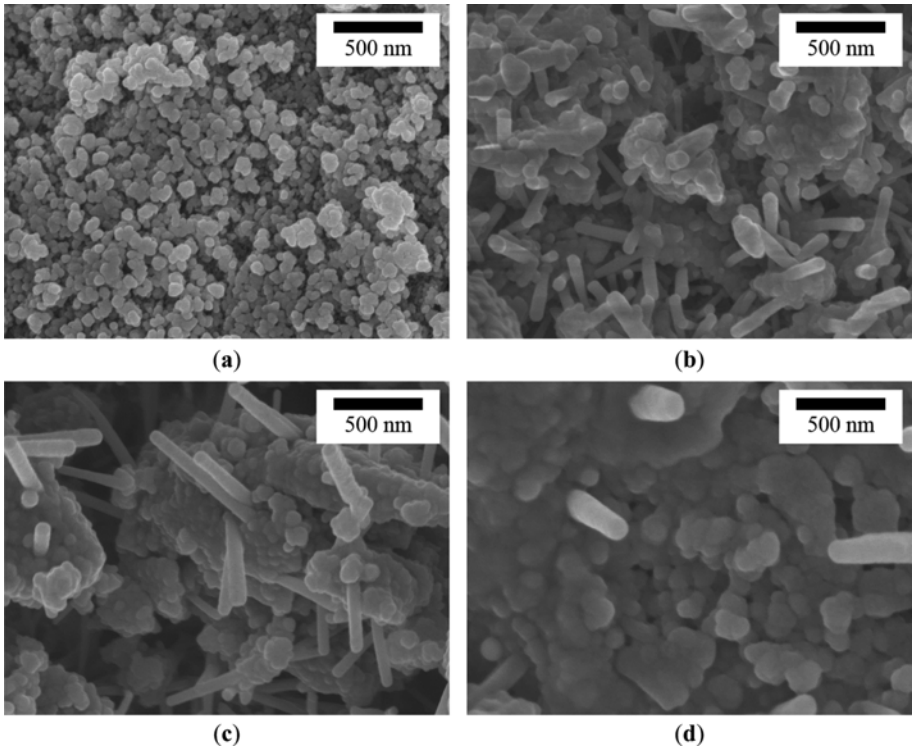

Fig. 9. SEM images of (a) alumina calcined at 950 °C, (b) KAl(D)I30T, (c) KAl(D)I40T and (d) KAl(D)I50T sorbents (scale bars=500 nm).

at 1 cycle, respectively. These values were maintained over the course of multiple cycles, even though the initial CO_2 capture capacity decreased slightly with the CO_2 thermal treatment. These results indicate that only $KHCO_3$ was formed during the CO_2 sorption, without any by-products. As the bare δ-alumina with CO_2 thermal treatment had no CO_2 capture capacity, its data was excluded. Based on these results, we suggest that the deactivation of a potassium-based alumina sorbent could be completely resolved by the use of the CO_2 thermal treatment method. Fig. 11(a) shows the CO_2 capture capacities and amount of CO_2 sorption per gram of sorbent of the KAl(D)I40T sorbents at 1 and 5 cycles as a function of the K_2CO_3 loading in the presence of 1 vol% CO_2 and 10 vol% H_2O at 60 °C. The K_2CO_3 contents of the KAl(D)I30T, KAl(D)I40T and KAl(D)I50T sorbents were determined by using an ICP-AES analysis. Table 3 lists the K_2CO_3 loadings of the potassium-based

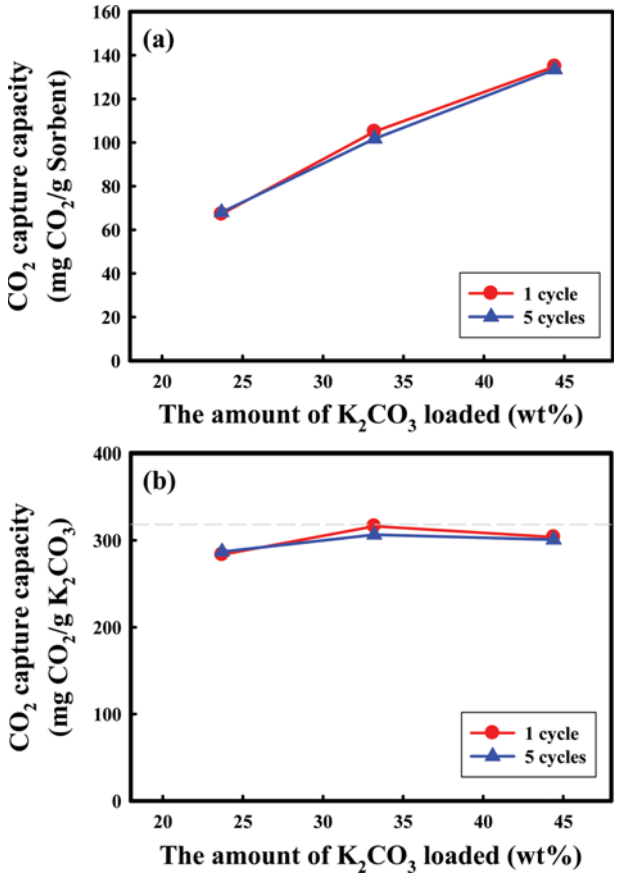

Fig. 11. CO_2 capture capacities in the presence of 1 vol% CO_2 and 10 vol% H_2O at 60 °C (a) per gram of sorbent and (b) per gram of K_2CO_3 as a function of K_2CO_3 loading.

Table 3. ICP-AES results for potassium-based alumina sorbents with and without CO_2 thermal treatment

Sample name	Amount of K_2CO_3 loaded (wt%)	Sample name	Amount of K_2CO_3 loaded (wt%)
KAl(D)I30	30.3	KAl(D)I30T	23.7
KAl(D)I40	40.3	KAl(D)I40T	33.2
KAl(D)I50	50.6	KAl(D)I50T	44.4

δ-alumina sorbents with and without the CO_2 thermal treatment. Aqueous solutions of K_2CO_3 were used to measure the actual K_2CO_3 loading with the ICP-AES analysis because it is easily dissolved in deionized water, whereas $KAl(CO_3)(OH)_2$ is insoluble. The K_2CO_3 loadings of the KAl(D)I30, KAl(D)I40 and KAl(D)I50 sorbents were 30, 40 and 50 wt%, respectively, which showed great similarity to the amount of K_2CO_3 impregnated. In the cases of KAl(D)I30T, KAl(D)I40T and KAl(D)I50T, the loading amounts were much lower than those of the sorbents without the CO_2 thermal treatment, at 23.7, 33.2 and 44.4 wt%, respectively. This was a result of the CO_2 thermal treatment converting some of the K_2CO_3 into $KAl(CO_3)(OH)_2$, which reduced the amount of K detectable using ICP-AES. Fig. 11(b) shows the CO_2 capture capacities and amounts of CO_2 sorption per gram of K_2CO_3 of the KAl(D)I40T sorbent at 1 and 5 cycles as a function of the K_2CO_3 loading in the presence of 1 vol% CO_2 and 9 vol% H_2O at 60 °C. As shown in Fig. 11(a), the CO_2 capture capacities of the sorbents increased in proportion to the K_2CO_3 loading. Additionally, the CO_2 capture capacities remained stable over five cycles, indicating excellent regenerability. It was also confirmed that the CO_2 capture capacities of these sorbents at 1 cycle and 5 cycles were equivalent to approximately 88-99% of their theoretical values (318.8 mg CO_2/g K_2CO_3), as calculated from the number of moles of K_2CO_3 loaded in the sorbents.

Fig. 12 shows the XRD patterns of the KAl(D)I30T, KAl(D)I40T and KAl(D)I50T sorbents after CO_2 sorption at 60 °C. These XRD patterns show the δ-alumina, $KAl(CO_3)(OH)_2$ and $KHCO_3$ peaks (JCPDS No. 70-0995). In these XRD patterns, the $K_2CO_3 \cdot 1.5H_2O$

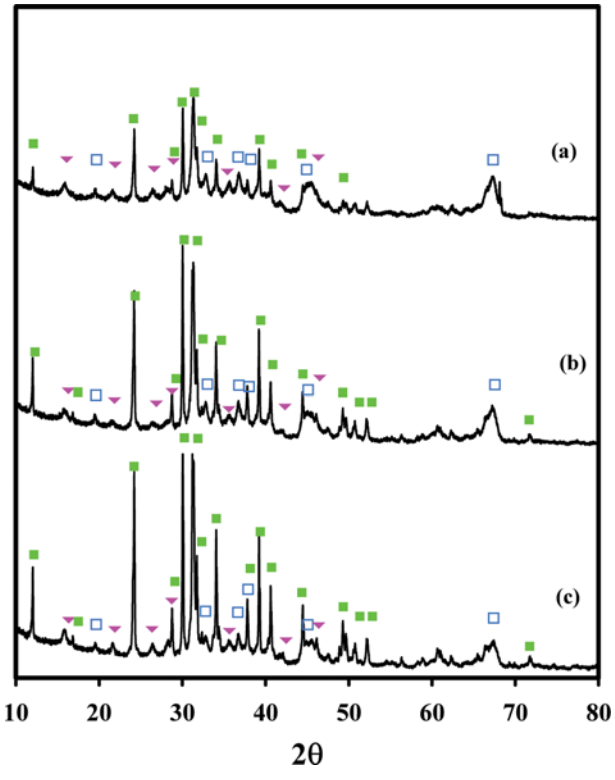

Fig. 12. XRD patterns of (a) KAl(D)I30T, (b) KAl(D)I40T and (c) KAl(D)I50T sorbents after CO_2 sorption; (□) δ-Al_2O_3; (■) $KHCO_3$; (▼) $KAl(CO_3)(OH)_2$.

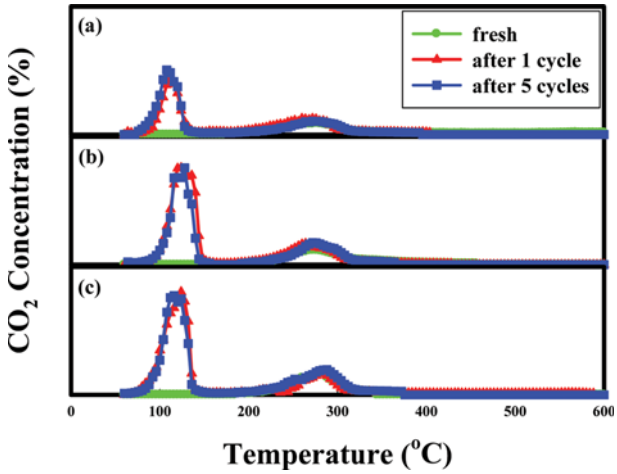

Fig. 13. TPD profiles of (a) KAl(D)I30T, (b) KAl(D)I40T and (c) KAl(D)I50T sorbents before and after CO_2 sorption.

was completely converted into $KHCO_3$. To confirm the effects of the CO_2 thermal treatment, TPD experiments were carried out on sorbents such as KAl(D)I30T, KAl(D)I40T and KAl(D)I50T before and after CO_2 sorption at 1 and 5 cycles by measuring the concentration of CO_2 desorbed when the temperature was ramped at a rate of 1 °C/min. These results, in Fig. 13, show that for fresh sorbent, only one peak was observed at around 270 °C, which resulted from the $KAl(CO_3)(OH)_2$ produced by the CO_2 thermal treatment. On the other hand, in the cases of the sorbents after CO_2 sorption at 1 and 5 cycles, two CO_2 peaks were observed at around 130 °C and 270 °C. The key observation from the TPD results is that the peak areas of these sorbents after 1 and 5 cycles were similar to those of the fresh sorbent, with the exception of the peak found at 130 °C, which resulted from the conversion of $K_2CO_3 \cdot 1.5H_2O$ to $KHCO_3$. This means that the potassium-based alumina sorbents developed in this study could be completely regenerated even at 130 °C.

CONCLUSION

The CO_2 sorption and regeneration properties of δ-alumina sorbents prepared by the impregnation of δ-alumina with K_2CO_3 were evaluated. The potassium-based alumina sorbents were not completely regenerated at 200 °C because of the formation of the by-product $[KAl(CO_3)(OH)_2]$, even though the deactivation of these sorbents was alleviated by increasing the K_2CO_3 loading. To overcome this deactivation problem, a new potassium-based alumina sorbent was developed using a CO_2 thermal treatment in the presence of 10 vol% CO_2 and 10 vol% H_2O. These new potassium-based alumina sorbents maintained their CO_2 capture capacities over multiple cycles, even though the initial CO_2 capture capacity was slightly decreased by the CO_2 thermal treatment. The excellent regeneration properties of these potassium-based alumina sorbents prepared using the CO_2 thermal treatment were due to the formation of $KHCO_3$ without a by-product during the CO_2 sorption. Based on these results, we conclude that the problem with the deactivation of potassium-based alumina sorbents can be solved by CO_2 thermal treatment.

ACKNOWLEDGEMENTS

We acknowledge the financial support by grants from Korea CCS R&D Center, funded by the Ministry of Education, Science and Technology of Korean government (NRF-2014M1A8A1049249). This research was supported by Kyungpook National University Research Fund, 2012.

REFERENCES

1. D. W. Keith, *Science*, **325**, 5948 (2009).
2. D. Aaron and C. Tsouris, *Sep. Sci. Technol.*, **40**, 321 (2005).
3. D. J. Hofmann, J. H. Butler and P. P. Tans, *Atomos. Environ.*, **43**, 2084 (2009).
4. D. P. Hagewiesche, S. S. Ashour, H. A. Al-Ghawas and O. C. Sandall, *Chem. Eng. Sci.*, **50**, 1071 (1995).
5. Z. Yong, V. Mata and A. E. Rodrigues, *J. Chem. Eng. Data*, **45**, 1093 (2000).
6. R. V. Siriwardane, M.-S. Shen, E. P. Fisher and J. A. Poston, *Energy Fuels*, **15**, 279 (2001).
7. Z. Yong, V. Mata and A. E. Rodrigues, *Ind. Eng. Chem. Res.*, **40**, 204 (2001).
8. Y. Takamura, S. Narita, J. Aoki, S. Hironaka and S. Uchida, *Sep. Purif. Technol.*, **24**, 519 (2001).
9. Z. Yong, V. Mata and A. E. Rodrigues, *Adsorption*, **7**, 41 (2001).
10. Z. Yong and A. E. Rodrigues, *Adsorpt. Sci. Technol.*, **19**, 255 (2001).
11. Z. Yong and A. E. Rodrigues, *Energy Convers. Manage.*, **43**, 1865 (2002).
12. Z. Yong, V. Mata and A. E. Rodrigues, *Sep. Purif. Technol.*, **26**, 195 (2002).
13. M. Mavroudi, S. P. Kaldis and G. P. Sakellaropoulos, *Fuel*, **82**, 2153 (2003).
14. C. Shen, C. A. Grande, P. Li, J. Yu and A. E. Rodrigues, *Chem. Eng. J.*, **160**, 398 (2010).
15. A. Sayari, Y. Belmabkhout and R. Serna-Guerrero, *Chem. Eng. J.*, **171**, 760 (2011).
16. J. A. Thompson, J. T. Vaughn, N. A. Brunelli, W. J. Koros, C. W. Jones and S. Nair, *Micro. Meso. Mater.*, **192**, 43 (2014).
17. G. Sethia and A. Sayari, *Carbon*, **93**, 68 (2015).
18. S. Hirano, N. Shigemoto, S. Yamada and H. Hayashi, *Bull. Chem. Soc. Jpn.*, **68**, 1030 (1995).
19. H. Hayashi, J. Taniuchi, N. Furuyashiki, S. Sugiyama, S. Hirano, N. Shigemoto and T. Nonaka, *Ind. Eng. Chem. Res.*, **37**, 185 (1998).
20. H. Gupta and L.-S. Fan. *Ind. Eng. Chem. Res.*, **41**, 4035 (2002).
21. E. L. G. Oliveira, C. A. Grande and A. E. Rodrigues, *Sep. Purif. Technol.*, **62**, 137 (2008).
22. Y. Liang, D. P. Harrison, R. P. Gupta, D. A. Green and W. J. McMichael, *Energy Fuels*, **18**, 569 (2004).
23. N. Shigemoto, T. Yanagihara, S. Sugiyama and H. Hayashi, *Energy Fuels*, **20**, 721 (2006).
24. Y. Seo, S.-H. Jo, C. K. Ryu and C.-K. Yi, *Cheomosphere*, **69**, 712 (2007).
25. J. B. Lee, C. K. Ryu, J.-I. Baek, J. H. Lee, T. H. Eom and S. H. Kim, *Ind. Eng. Chem. Res.*, **47**, 4465 (2008).
26. A. Samanta, A. Zhao, G. K. H. Shimizu, P. Sarkar and R. Gupta, *Ind. Eng. Chem. Res.*, **51**, 1438 (2012).

27. Y. K. Park, H. Seo, W. C. Choi, N. Y. Kang, S. Park, D. Y. Min, K. Kim, K. S. Lee, H. K. Moon, H. H. Cho and D. K. Lee, *Energy Procedia*, **63**, 2266 (2014).
28. Y. C. Park, S.-H. Jo, D.-H. Kyung, J.-Y. Kim, C.-K. Yi, C. K. Ryu and M. S. Shin, *Energy Procedia*, **63**, 2261 (2014).
29. K.-C. Kim, Y. C. Park, S.-H. Jo and C.-K. Yi, *Korean J. Chem. Eng.*, **28**, 1986 (2011).
30. K. Kim, S. Yang, J. B. Lee, T. H. Eom, C. K. Ryu, H.-J. Lee, T.-S. Bae, Y.-B. Lee and S.-J. Lee, *Korean J. Chem. Eng.*, **32**, 667 (2015).
31. A. G. Okunev, V. E. Sharonov, Y. I. Aristov and V. N. Parmon, *React. Kinet. Catal. Lett.*, **71**, 355 (2000).
32. C. K. Yi, S. H. Jo, H. J. Ryu, Y. W. Yoo, J. B. Lee and C. K. Ryu, *Greenhouse Gas Control Technologies 7*, **2**, 1765 (2005).
33. D. P. Harrison, *Greenhouse Gas Control Technologies 7*, **2**, 1101 (2005).
34. C. Zhao, X. Chen and C. Zhao, *Chemosphere*, **75**, 1401 (2009).
35. C. Zhao, X. Chen, C. Zhao and Y. Liu, *Energy Fuels*, **23**, 1766 (2009).
36. S. C. Lee, H. J. Chae, S. J. Lee, Y. H. Park, C. K. Ryu, C. K. Yi and J. C. Kim, *J. Mol. Catal. B: Enzym.*, **56**, 179 (2009).
37. C. K. Yi, S. H. Jo, Y. Seo, J. B. Lee and C. K. Ryu, *Int. J. Greenhouse Gas Control*, **1**, 31 (2007).
38. Q. Wang, J. Luo, Z. Zhong and A. Borgna, *Energy Environ. Sci.*, **4**, 42 (2011).
39. S. C. Lee, B. Y. Choi, T. J. Lee, C. K. Ryu, Y. S. Ahn and J. C. Kim, *Catal. Today*, **111**, 385 (2006).
40. S. C. Lee, M. S. Cho, S. Y. Jung, C. K. Ryu and J. C. Kim, *Adsorption*, **20**, 331 (2014).
41. S. C. Lee, Y. M. Kwon, H. J. Chae, S. Y. Jung, J. B. Lee, C. K. Ryu, C. K. Yi and J. C. Kim, *Fuel*, **104**, 882 (2013).
42. S. C. Lee, B. Y. Choi, C. K. Ryu, Y. S. Ahn, T. J. Lee and J. C. Kim, *Korean J. Chem. Eng.*, **23**, 374 (2006).
43. C. Zhao, X. Chen and C. Zhao, *Energy Fuels*, **26**, 1395 (2012).
44. W. Dong, X. Chen, F. Yu and Y. Wu, *Energy Fuels*, **29**, 968 (2015).
45. S. C. Lee, H. J. Chae, S. J. Lee, B. Y. Choi, C. K. Yi, J. B. Lee, C. K. Ryu and J. C. Kim, *Environ. Sci. Technol.*, **42**, 2736 (2008).
46. W. Dong, X. Chen and Y. Wu, *Energy Fuels*, **28**, 3310 (2014).
47. C. Zhao, X. Chen and C. Zhao, *Energy Fuels*, **26**, 1406 (2012).
48. L. Li, Y. Li, X. Wen, F. Wang, N. Zhao, F. Xiao, W. Wei and Y. Sun, *Energy Fuels*, **25**, 3835 (2011).
49. J. V. Veselovskaya, V. S. Derevshikov, T. Y. Kardash, O. A. Stonkus, T. A. Trubitsina and A. G. Okunev, *Int. J. Greenhouse Gas Control*, **17**, 332 (2013).
50. S. Bali, M. A. Sakwa-Novak and C. W. Jones, *Colloids Surf. A Physicochem. Eng. Asp.*, **486**, 78 (2015).
51. S. C. Lee, Y. M. Kwon, C. Y. Ryu, H. J. Chae, D. Ragupathy, S. Y. Jung, J. B. Lee, C. K. Ryu and J. C. Kim, *Fuel*, **90**, 1465 (2011).